Available online at www.sciencedirect.com
SCIENCE DIRECT
Geochimica et Cosmochimica Acta 70 (2006) 277–289
Geochimica
www.elsevier.com/locate/gca

Kinetic isotopic fractionation during diffusion of ionic species in water

Frank M. Richter [a,*], Ruslan A. Mendybaev [a], John N. Christensen [b], Ian D. Hutcheon [c], Ross W. Williams [c], Neil C. Sturchio [d], Abelardo D. Beloso Jr. [d]

[a] The University of Chicago, Department of the Geophysical Sciences, 5734 South Ellis Avenue, Chicago, IL 60637, USA
[b] Lawrence Berkeley National Laboratory, Berkeley, CA, USA
[c] Glenn T. Seaborg Institute, Lawrence Livermore National Laboratory, Livermore, CA, USA
[d] University of Illinois at Chicago, Chicago, IL 60607, USA

Received 10 June 2005; accepted in revised form 12 September 2005

Abstract

Experiments specifically designed to measure the ratio of the diffusivities of ions dissolved in water were used to determine D_{Li}/D_K, $D_{^7Li}/D_{^6Li}$, $D_{^{25}Mg}/D_{^{24}Mg}$, $D_{^{26}Mg}/D_{^{25}Mg}$, and $D_{^{37}Cl}/D_{^{35}Cl}$. The measured ratio of the diffusion coefficients for Li and K in water ($D_{Li}/D_K = 0.6$) is in good agreement with published data, providing evidence that the experimental design being used resolves the relative mobility of ions with adequate precision to also be used for determining the fractionation of isotopes by diffusion in water. In the case of Li, we found measurable isotopic fractionation associated with the diffusion of dissolved LiCl ($D_{^7Li}/D_{^6Li} = 0.99772 \pm 0.00026$). This difference in the diffusion coefficient of ^{7}Li compared to ^{6}Li is significantly less than that reported in an earlier study, a difference we attribute to the fact that in the earlier study Li diffused through a membrane separating the water reservoirs. Our experiments involving Mg diffusing in water found no measurable isotopic fractionation ($D_{^{25}Mg}/D_{^{24}Mg} = 1.00003 \pm 0.00006$). Cl isotopes were fractionated during diffusion in water ($D_{^{37}Cl}/D_{^{35}Cl} = 0.99857 \pm 0.00080$) whether or not the co-diffuser (Li or Mg) was isotopically fractionated. The isotopic fractionation associated with the diffusion of ions in water is much smaller than values we found previously for the isotopic fractionation of Li and Ca isotopes by diffusion in molten silicate liquids. A major distinction between water and silicate liquids is that water surrounds dissolved ions with hydration shells, which very likely play an important but still poorly understood role in limiting the isotopic fractionation associated with diffusion.

1. Introduction

Mass-dependent kinetic isotope fractionation during chemical diffusion is a well-known phenomenon in gases and certain liquids. In the case of an ideal gas at sufficiently low pressure such that collisions are infrequent, kinetic theory predicts that the ratio of the diffusion coefficients of two gaseous species will be proportional to the inverse square root of their molecular mass, which we can write as

$$\frac{D_1}{D_2} = \left(\frac{m_2}{m_1}\right)^{\beta}, \quad (1)$$

where D_1 and D_2 are the diffusion coefficients of gas species of molecular weight m_1 and m_2, and $\beta = 0.5$. The more common situation of geochemical interest is that of isotope fractionation of a dilute gas diffusing through a different gas of finite pressure. A classic version of this can be found in Craig and Gordon's (1965) discussion of the relative rates of diffusion of $H_2{}^{16}O$, $HD^{16}O$, and $H_2{}^{18}O$ vapor in air. Taking collisions into account while still assuming that intermolecular forces are negligible, the ratio of the diffusion coefficients of the isotopically distinct species becomes proportional to the inverse square root of their reduced mass. The reduced mass μ_i of a species of molecular weight m_i colliding with a gas of molecular weight M is given by the expression

* Corresponding author.
E-mail address: richter@geosci.uchicago.edu (F.M. Richter).

0016-7037/$ - see front matter © 2005 Elsevier Inc. All rights reserved.
doi:10.1016/j.gca.2005.09.016

$$\mu_i = \frac{m_i M}{m_i + M}. \quad (2)$$

The ratio of the diffusion coefficients of the dilute isotopically distinct molecules is then given by

$$\frac{D_1}{D_2} = \sqrt{\frac{\mu_2}{\mu_1}} = \sqrt{\frac{m_2(m_1+M)}{m_1(m_2+M)}}. \quad (3)$$

An interesting point is that when the molecular weight M of the medium is very large compared to that of the diffusing species, $\mu_i \to m_i$ as $m_i/M \to 0$, and the ratio of the diffusion coefficients reverts to that given by Eq. (1). Eqs. (1) and (3) provide an upper bound on mass-dependent kinetic isotope fractionation by diffusion in gases and serve as a point of comparison for the magnitude of fractionations observed in condensed systems. It should be kept in mind that even in the case of gases these relationships make a number of simplifying assumptions such as that the gas medium can be represented by its mean molecular weight, that intermolecular forces are negligible, and that differences in the molecular diameters of the diffusing species are not significant. Despite these simplifications, Eq. (3) was shown by Craig and Gordon (1965) to be in reasonably good agreement with experimental data on the isotopic fractionation of water vapor diffusing in air. While there is no theoretical expectation as to the value of β in Eq. (1) for anything other than dilute gases, we will nevertheless use β as a convenient way of specifying and comparing the mass-dependence of isotopic fractionations during diffusion in a variety of condensed systems.

The understanding of mass-dependent fractionation by diffusion in condensed systems is far less developed than for gases. Even such apparently simple situations as those involving the isotopic fractionation of dissolved trace gases (e.g., He, methane, and CO_2) in water have not yielded unambiguous results (see for example, Jähne et al., 1987; Prinzhofer and Pernaton, 1997; Zhang and Krooss, 2001). Jähne et al. (1987) carried out experiments to determine the relative diffusivities of noble gases dissolved in water at various temperatures and found that the ratios of the diffusion coefficients of the noble gases are very close to the inverse square root of the mass of the noble gases (i.e., $\beta = 0.5$ in Eq. (1)). In some cases, the experimental results for the relative diffusion coefficients of the noble gases in water imply β slightly greater than 0.5, a surprising result suggesting that interpreting the diffusion coefficients in terms of mass alone is not entirely correct. An alternative interpretation of the noble gas data is that the diffusion coefficients of neutral species are dominated by hydrodynamic drag (as indicated by the molecular calculations of Koneshan et al., 1998), in which case the diffusivity will be inversely proportional to the size. If we use the van der Waals radius as a measure of the relative sizes of the diffusing noble gases, then diffusion coefficients that are inversely proportional to size will appear to depend on the inverse square root of mass because of the close to linear correlation between the square root of the mass and the Van der Waals radius of noble gases other than helium. The most direct way of isolating the effect of mass on diffusion is to compare the behavior of isotopically substituted species. Jähne et al. (1987) also report on two experiments that were used to determine isotopic fractionation of dissolved $^{12}CO_2$ from $^{13}CO_2$ and ^3He from ^4He. The results for CO_2 showed an isotopic fractionation more than an order of magnitude less than what one calculates assuming that diffusivities are proportional to the inverse square root of the mass ratio of $^{12}CO_2/^{13}CO_2$ (i.e., $\sqrt{\frac{44}{45}}$). Jähne et al. (1987) discuss their measured isotopic fractionation in terms of an expectation based on the inverse square root of the reduced masses using the molecular weight of water for M in Eq. (2) (i.e., $\mu_{^{13}CO_2} = 12.86$ and $\mu_{^{12}CO_2} = 12.77$). The measured fractionation of carbon isotopes is then about one-third the value calculated from the inverse square root of the ratio of the reduced mass. Why a reduced mass derived from the kinetic theory of gases should be applicable to the behavior of dissolved trace gases in water is not explained. The fractionation of He isotopes reported by Jähne et al. (1987) corresponds to $D_{^3He}/D_{^4He} = 1.15 \pm .03$, which, given the uncertainty, is indistinguishable from the ratio calculated using the actual mass of the He isotopes (1.16) or that calculated using the reduced mass based on the molecular weight of water (1.13). The upshot of all this is that the effect of mass on the diffusion of neutral species in water is not at all simple, and it is not yet well documented or understood.

The work we report here focuses on the isotopic fractionation of dissolved ionic species in water. Because one of the principal applications we hoped to explore was the development of an isotopic monitor for the diffusive transport of mineral-forming solutes in water saturated sedimentary or metamorphic systems, we focused on dissolved ionic species rather than trace gases. Another context where isotopic fractionation during diffusive transport of ionic species in water could be very important involves biological systems, where isotopic fractionation has been measured, but remains poorly understood. For example, a recent interpretation of calcium isotopic fractionation during inorganic aragonite precipitation and in cultured foraminifera (Gussone et al., 2003) includes kinetic effects due to diffusion in water, but for the moment this is still in the realm of speculation due to the lack of relevant experimental data on the degree of isotopic fractionation produced during the diffusion of ions in water.

Previous work led us to expect that we might find large mass-dependent isotopic fractionation of dissolved ions as they diffuse in water. We recently demonstrated significant mass dependent isotopic fractionation by diffusion in molten silicate liquids (Richter et al., 1999, 2003), which when phrased in terms of the exponent β in Eq. (1), resulted in $\beta \approx 0.2$ for lithium isotopes and $\beta \approx 0.1$ for calcium isotopes. If diffusion in complex molten silicate liquids can produce such large isotopic fractionation, why would not

diffusion in water? Another reason for us to expect that we might find significant isotopic fractionation during diffusion of ions in water was the report by Fritz (1992) of large isotopic fractionation of lithium during the diffusion of dissolved LiCl. Fritz (1992) interpreted his measurements as indicating a mass dependence of lithium diffusion in water corresponding to $D_{^6LiCl}/D_{^7LiCl} = 1.011 \pm 0.003$, which, he noted, is very close to the inverse square root of the mass ratio of ^{6}LiCl and ^{7}LiCl (i.e., Eq. (1) with $m_1 = 40$, $m_2 = 41$, and $\beta = 0.5$). Leaving aside that Fritz (1992) gave no reason why one should expect these masses to be the relevant masses for the diffusing species or for the choice of $\beta = 0.5$, the fact that he reported large fractionation of Li isotopes as they diffused in water led us to expect that we might find similar effects. On the other hand, an earlier report by Kunze and Fuoss (1962) found significantly less Li isotope fractionations (see Table 1) based on the relative conductances of ^{6}Li and ^{7}Li in water.

The Li isotope fractionations we measured are a factor of 5 less than that implied by the results given by Fritz (1992) and much closer to those reported by Kunze and Fuoss (1962). In the case of Mg diffusing in water, the isotopic fractionation is below our detection limits. To the extent that the lack of measurable kinetic isotope effects for Mg can be used to infer similar behavior for Ca, the appeal by Gussone et al. (2003) to significant Ca isotope fractionation by diffusion in water seems unjustified. We found measurable fractionations of Cl isotopes regardless of whether the co-diffuser, Li or Mg, was isotopically fractionated.

2. Experimental design

A sketch of the experimental design we used is shown in Fig. 1. The basic design is not much different from that used by Thomas Graham (1805–1869) in his classic studies of effusion that led to what is generally known as Graham's law of effusion (Eq. (1)). In our version of Graham's experiment, two nested glass containers of very different volume are connected by a small cylindrical tube through which a dissolved salt, initially only in the smaller inner container, diffuses into the larger outer container. The dimensions were chosen such that the time for significant diffusion to take place between containers (tens of days) is long compared to the time of a few days it takes for diffusion to maintain an effectively homogeneous distribution of salt in the smaller inner container. Under these circumstances, the flux J_i of a dissolved component from the inner container to the larger outer one will be governed to a reasonably good approximation by

$$J_i = \frac{D_i A (C_{i,1} - C_{i,2})}{L}, \tag{4}$$

where D_i is the diffusion coefficient for the dissolved component i, $C_{i,1}$ and $C_{i,2}$ are the molar densities of i (i.e., moles of i per unit volume) in the inner and outer containers, respectively, and A and L are the inner cross-sectional area and length of the connecting tube. The evolution of the molar density is governed by

Table 1
Parameters for elemental and isotopic fractionation by diffusion in water and in silicate liquids

Parameters for elemental and isotopic fractionation by diffusion in water				
Species	D_i/D_j	$\pm 2\sigma$	β in Eq. (1)	Source
Noble gases	$D_i/D_j = (m_i/m_j)^{1/2}$		~0.5	Jähne et al. (1987)
Li/K	$D_{Li}/D_K = 0.598$	0.006		This work, Fig. 2
	$D_{Li}/D_K = 0.58$[a]	~0.02[b]		Robinson and Stokes (1959)
Fe isotopes (0.33 M HNO_3)	$D_{^{56}Fe}/D_{^{54}Fe} = 0.999914$	Not given	0.0024	Rodushkin et al. (2004)
Zn isotopes (0.84 M HNO_3)	$D_{^{66}Zn}/D_{^{64}Zn} = 0.999942$	Not given	0.0019	Rodushkin et al. (2004)
Na isotopes	$D_{^{24}Na}/D_{^{22}Na} = 0.998$	~0.002[c]	0.023	Pikal (1972)
Li isotopes	$D_{^7Li}/D_{^6Li} = 0.99772$	0.00026	0.015	This work, Fig. 5
	(0.9890)	(0.003)	(0.071)	(Fritz, 1992)
	(0.9965)	~0.002[d]	(0.023)	(Kunze and Fuoss, 1962)
Mg isotopes	$D_{^{25}Mg}/D_{^{24}Mg} = 1.00003$	0.00006	~0	This work, Fig. 4
Cl isotopes	$D_{^{37}Cl}/D_{^{35}Cl} = 0.99857(0.9981–0.9986)$	0.00080	0.025	This work, Fig. 7(Coleman et al., 2000)

Parameters for elemental and isotopic fractionation by diffusion in silicate liquids				
Species	D_i/D_j	β in Eq. (1)	Range of β	Source (Richter et al., 2003)
Li/K	$D_{Li}/D_K \sim 1000$			Rhyolite melt
	$D_{Li}/D_K \sim 100$			Basalt melt
Li isotopes	$D_{^7Li}/D_{^6Li} = 0.9674$	0.215	0.015	Rhyolite-basalt interdiffusion
Ca isotopes	$D_{^{44}Ca}/D_{^{40}Ca} = 0.9929$	0.075	0.025	Rhyolite-basalt interdiffusion

[a] Value for 75 °C based on the best fitting line through the ratio of the limiting equivalent conductivities of Li and K as a function of temperature given by Robinson and Stokes (1959) in Appendix 6.2.
[b] Estimate based on the goodness of fit of a straight line through the ratio of the limiting equivalent conductivity data of Li and K.
[c] Estimated from data in Table 1 of Pikal (1972).
[d] Estimated from data in Table IV of Kunze and Fuoss (1962).

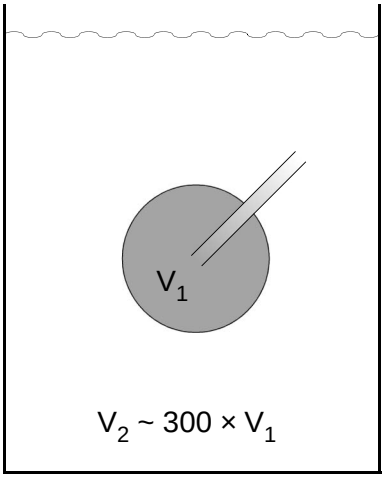

Fig. 1. Schematic diagram of the experimental apparatus used to measure the relative diffusivity of ionic species dissolved in water. The small(source) containers that we used have interior volumes between 0.5 and 0.7 cm^3 while the outer(sink) container is filled with approximately 200 ml water. The diffusion tube connecting the two chambers has a nominal inner diameter of 1 mm and a length of either 0.8 or 1.2 cm. The different lengths were used to verify that the length of the connecting tube and the associated time constant for diffusive exchange did not affect the relative diffusivity measurements. The source containers were suspended in such a way that the diffusion tube was at about 45° from the vertical to facilitate the denser salty fluid falling away from the tip of the diffusion tube.

$$\frac{\partial C_{i,N}}{\partial t} = -\frac{J_i}{V_N}, \tag{5}$$

where V is the container volume, the subscript N indicates the container to which the equation is applied ($N = 1$ for inner "source" container, $N = 2$ for outer "sink" container). The flux J_i is positive if directed out of the container to which the equation is applied. We designed the experiment in such a way that $V_2 \gg V_1$ in order that changes in the molar density of the outer container would be negligible (except at very long times) compared to changes in the much smaller inner container. The initial conditions for most of our experiments were $C_{i,1} = C_{i,o}$ and $C_{i,2} = 0$. The solution to Eq. (5) that will be valid until such time that $C_{i,2}$ is no longer negligible compared to $C_{i,1}$ is

$$C_{i,1} = C_{i,o} e^{-(D_i A/V_1 L)t}. \tag{6}$$

The evolution with time of the ratio $R_{ij} = C_{i,1}/C_{j,1}$ of the molar densities of elemental or isotopically distinct components i and j in the source container is then

$$R_{ij} = R_{ij,o} e^{-(D_j A/V_1 L)t(\frac{D_i}{D_j}-1)}, \tag{7}$$

where $R_{ij,o}$ is the initial ratio. Recognizing that the quantity $e^{-(D_j A/V_1 L)t}$ in Eq. (7) is the fraction f_j of component j remaining in the inner source container and taking the natural logarithm of both sides of Eq. (7), we can write

$$\ln\left(\frac{R_{ij}}{R_{ij,o}}\right) = \left(\frac{D_i}{D_j} - 1\right) \ln f_j. \tag{8}$$

The advantages of the present experimental design can now be seen in Eqs. (7) and (8). Eq. (7) shows that the isotopic fractionation of the salt remaining in the source container increases exponentially with time for $D_i < D_j$, and thus, even small differences in the diffusivity of isotopically distinct species can produce measurable effects because of this exponential amplification. Eq. (8) shows that a set of measurements of R_{ij} and f_j taken from experiments of different duration should, when plotted as $\ln(R_{ij}/R_{ij,o})$ versus $-\ln f_j$, fall along a straight line of slope $(1 - \{D_i/D_j\})$. Finding that the data fall along such a line serves as a check that the experiment is in fact behaving as expected and also provides a measure of D_i/D_j from the slope of the best fitting line through the data.

It should be noted that while our experimental design is appropriate for measuring small differences between diffusion coefficients, it is not particularly well suited for making equivalently high-precision determinations of the diffusion coefficients individually. Accurate determinations of individual diffusion coefficients would require a far greater uniformity in the geometry of the various source chambers that we used and a much more detailed accounting of how the flux depends on the geometry of the system than implied by Eq. (4). However as shown by Eq. (8), the details of the geometry of the system cancel when results are given in terms of the ratio of diffusion coefficients.

The ionic salts used in this study are KCl, LiCl, $CaCl_2$, and $MgCl_2$. A set of validation experiments were run in which mixtures of KCl and LiCl were allowed to diffuse out of the source container. Both the K/Li and the fraction of potassium remaining in the source container were measured and the data from the various experiments were used in connection with Eq. (8) to determine D_{Li}/D_K. Our finding that the diffusivity ratio determined in this way is in good agreement with previously published data on the diffusivity of these two cations in water would be evidence that our experimental design does fractionate dissolved cations in proportion to their relative diffusivities. The isotopic ratios we measured were $^7Li/^6Li$ in solutions from diffusion experiments involving LiCl, $^{25}Mg/^{24}Mg$ and $^{26}Mg/^{24}Mg$ in the solutions from $MgCl_2$ experiments, and $^{37}Cl/^{35}Cl$ in solutions from a subset of the LiCl and $MgCl_2$ experiments. In some of the diffusion experiments involving $MgCl_2$, the water in the outer container had an approximately equal molar concentration of $CaCl_2$ as the initial concentration of $MgCl_2$ in the source chamber. This was done so that Mg^{2+} could exchange with Ca^{2+} without much Cl^- having to diffuse to maintain elecroneutrality. In a few instances, 0.5% agarose gel was added to the water in the inner chamber as a way of suppressing any mass transfer by (non-diffusive) flow between the containers that might have affected experiments in which the solvent was pure water. We found no significant difference between experiments with and without Ca as a counterdiffuser or between those with and without the agarose. Most experiments were run at a constant temperature of 75 °C chosen because of our interest in solute transport in sedimentary pore waters. Experiments in which agarose was added to

the water had to be run at 38 °C in order for the agarose to remain a gel.

3. Analytical methods

Starting solutions were prepared by dissolving measured amounts of crystalline $CaCl_2$, $MgCl_2$, KCl, LiCl (all Puratronic grade, >99.99%, AlfaAesar) in distilled water, or in a few cases, distilled water with 0.5% agarose gel. The flasks were filled by submerging them in the starting solution and extracting the air from the flask using a length of Teflon microtubing attached to a 10 ml syringe. Flasks holding between 0.5 and 0.7 ml of starting solution were then suspended 2–3 cm below the waterline of individual containers filled with approximately 200 ml of distilled water (or $CaCl_2$ in the Mg–Ca counterdiffusion experiments). The containers were then sealed with teflon tape so as to minimize evaporation and held for various lengths of time at constant temperature in an Isotherm Incubator (Fisher Scientific). After a prescribed period of time, a container was removed from the incubator, the small source flask extracted, and its contents were transferred to a 2 ml sterile polypropylene vial for storage.

Concentrations of Li, K, Mg, and Ca in the starting materials and run products were measured by a Varian SpectrAA 220 atomic absorption spectrometer using an air–acetylene flame. Standards (from 0.1 to 10 ppm) were prepared from 1000 ppm (±1%) reference solutions (Mg, K, and Ca solutions from Fisher Scientific; Li from Acros Organics). The solutions taken from the experiments were diluted with distilled water to concentrations of <10 ppm. The amount of the sample solution and water was controlled volumetrically using 10, 40, and 200 μl pipettes as needed and double checked by weighing using a Mettler AE163 balance. In order to suppress ionization of K during the atomic absorption measurements, an amount of $CsNO_3$ solution with 10,000 ppm Cs (SPEX CertiPrep) was added to all standards and solutions taken from the KCl/LiCl diffusion experiments to make a final solution with 1000 ppm Cs. The intake system of AA spectrometer was flushed with 3% HNO_3 after each analysis to reduce contamination. A typical analysis involved a set of four or five measurements of the samples bracketed by a blank and measurements of one or two standards. In addition, all standards were analyzed at the start, middle, and end of each AA session.

A subset of the samples that had been measured by atomic absorption was also measured with much greater precision with an Agilent 4500 ICPMS. The calibration standards used for quantification of the ICPMS measurements were prepared from primary standards obtained from SPEX and contained 0, 10, 20, 50, and 100 ppbw of Mg. All standards and samples contained 10 ppbw Sc used as an internal standard to correct for instrument drift. Samples were diluted to fall within the calibration range of the standards. The calibration standard block was run before and after the samples and the average sensitivity for ^{24}Mg was used to quantify the concentration of the samples. The reported ICPMS data represent the average and standard deviations of duplicate analyses made on 2 separate days. The uncertainties assigned to the AA measurements based on repeated measurements are consistent with the comparability between the AA and the much more precise ICPMS concentration measurements.

The isotopic composition of Li in the experimental solutions was measured at Lawrence Berkeley National Laboratory using an IsoProbe (Micromass, now GV Instruments, Manchester, UK) multiple-collector ICP source sector mass spectrometer (MC-ICPMS). Ion beams of ^6Li and ^7Li were measured simultaneously with a pair of appropriately spaced Faraday cups. Sample and standard solutions were introduced to the IsoProbe using an Aridus (Cetac Technologies) desolvation system. To avoid background Li from the skimmer cone, ''soft'' extraction was used, where a positive potential is applied to the extraction lens. Helium was used in the collision cell to reduce the energy spread of the ion beam to $\leqslant 1$ eV before ion focusing and entry to the magnetic sector. Measurements of sample unknowns were bracketed with measurements of the LSVEC Li isotopic standard (NIST SRM 8545) and are reported relative to that standard (per mil deviation, δ^7Li). Analyses consist of 20 integrations at 5 s each for a total analysis time of ~100 s of a 1 ppm solution. This scheme uses ~100 ng of Li per analytical run. Both the standard and sample unknowns were diluted with 2% HNO_3 to the same concentration.

The magnesium isotopic composition of the experimental solutions was analyzed at Lawrence Livermore National Laboratory using a multi-collector ICPMS (IsoProbe, GV Instruments, Manchester, UK). The Mg was separated from other cations by ion exchange to minimize scattered ions and other ''matrix effects'' that act to change the magnitude of the instrumental mass bias. Recovery of Mg from the purification columns was determined to be greater than 98%. Samples and standards, dissolved in 2% HNO_3, were nebulized and transported to the plasma using an Aridus (Cetac Technologies) sample introduction system. For a given analytical session the standard solution was prepared to produce ^{24}Mg intensities of approximately 5×10^{-11} amps, and the samples were diluted to give ^{24}Mg intensities roughly equivalent to that of the standard. The ^{24}Mg, ^{25}Mg, and ^{26}Mg ion beams were measured simultaneously using Faraday cup detectors; integration times of 200 s were used to collect data. Pure 2% HNO_3 was analyzed before every sample to determine the instrument background at masses 24, 25, and 26 and net peak intensities for each Mg isotope were determined by subtracting the average on-peak intensities for pure HNO_3 from the following respective sample peak intensities. The background ion signal increased steadily with time due to buildup of contamination on the extraction optics; backgrounds were maintained at less than 0.05% of the sample signal by periodically replacing the cones and plasma torch. The background-corrected $^{25}Mg/^{24}Mg$ and $^{26}Mg/^{24}Mg$ ratios were corrected for instrumental mass

bias using the standard-sample-standard bracketing method (Galy et al., 2003). The reference sample for the Mg isotopic compositions reported here is DSM3 (Galy et al., 2003). The analyses were made relative to a standard solution prepared from NBS SRM 980, but during the course of this work the heterogeneous nature of the NBS material was discovered and subsequently reported in Galy et al. (2003). The LLNL SRM 980 solution was calibrated relative to the DSM3 standard solution and the data were corrected appropriately.

Stable Cl isotope ratios were measured at the Environmental Isotope Geochemistry Laboratory at the University of Illinois at Chicago using methods based on those described by Eggenkamp (1994) and Holt et al. (1997). An aliquot of the experimental solution containing ~3 mg of Cl was brought to a volume of 10 ml by evaporation or by adding deionized water (depending on sample concentration). Four milliliters of 1 M KNO_3 solution and 2 ml of 0.004 M $NaHPO_4$/0.107 M citric acid buffer were added to adjust the ionic strength and pH. The solution was gently heated to 80 °C and 3 ml of 0.38 M $AgNO_3$ was added to precipitate AgCl. The sample was then kept in a dark enclosure overnight. The AgCl precipitate was retrieved by centrifuging and washing three times with 0.1 M HNO_3. The AgCl precipitate was transferred into a 9-mm o.d. borosilicate glass tube that had been baked at 550 °C for 2 h. The tube was attached to a vacuum line for evacuation and cryogenic addition of 35 μl CH_3I. The tube was sealed and the contents were combusted at 300 °C for 2 h. The tube was then attached to a vacuum line, cracked open, and the released CH_3Cl was purified by cryogenic distillation using dry ice/acetone and pentane/liquid nitrogen slushes to regulate temperature. The purified CH_3Cl was cryogenically transferred using liquid nitrogen, measured manometrically, and sealed into another evacuated glass tube. The purified CH_3Cl was then introduced into the source of a Finnigan MAT Delta-Plus XL mass spectrometer for measurement of the ratio (m/z) 52/50. Measured ratios were normalized to those of aliquots of seawater Cl (Conception Bay, Newfoundland) prepared and measured by the same procedure (1–3 seawater samples per batch of 10 samples). Precision (1σ) of this analytical method is ±0.1‰.

4. Results

4.1. KCl–LiCl experiments

A series of experiments were run with LiCl + KCl in the source container and pure water in the outer container. The purpose of these experiments was to confirm that the experimental design produces concentration data that can be interpreted to give accurate relative diffusivities using Eq. (8). The LiCl and KCl concentrations in the starting solutions and in the waters from the inner container of experiments run for different lengths of time are given in an appendix. For the specific case considered here, Eq. (8) becomes

$$\ln\left(\frac{R_{\mathrm{Li,K}}}{R_{\mathrm{Li,K_o}}}\right) = \left(\frac{D_{\mathrm{Li}}}{D_{\mathrm{K}}} - 1\right)\ln f_{\mathrm{K}}, \tag{9}$$

where $R_{\mathrm{Li,K}}$ is the molar ratio of Li and K in the source container, $R_{\mathrm{Li,K_o}}$ is the initial ratio, $D_{\mathrm{Li}}/D_{\mathrm{K}}$ is the ratio of the diffusion coefficients of lithium and potassium in water, and f_{K} is the fraction of potassium remaining in the source container. As can be seen in Fig. 2, the data fall along a straight line until the concentration in the outer container begins to affect the fluxes. According to Eq. (9) the slope of this line corresponds to $(\{D_{\mathrm{Li}}/D_{\mathrm{K}}\} - 1)$, from which we find that $D_{\mathrm{Li}}/D_{\mathrm{K}} = 0.598 \pm 0.006$. The validation of our experimental design depends on how well this ratio compares with previously reported data on the diffusion of Li and K in water.

The diffusion matrix for the ternary system LiCl–KCl–H_2O has been measured by Leaist and Kanakos (2000) at 25 °C for a wide range of compositions and total molar concentrations in the range 0.5–3.0 M/dm^3. The off-diagonal terms in the diffusion matrix become smaller as the solutions become more dilute and for 0.5 M/dm^3 and equal molar densities of LiCl and KCl they are negligible for LiCl and about 10% of the diagonal coefficient for KCl. The concentrations of LiCl and KCl in the starting solutions of our experiments are about a factor of 5 less than lowest concentration used by Leaist and Kanakos (2000), and we can reasonably ignore off-diagonal terms in the diffusion matrix when using published data to compare to our results. We can then treat the system as being effectively

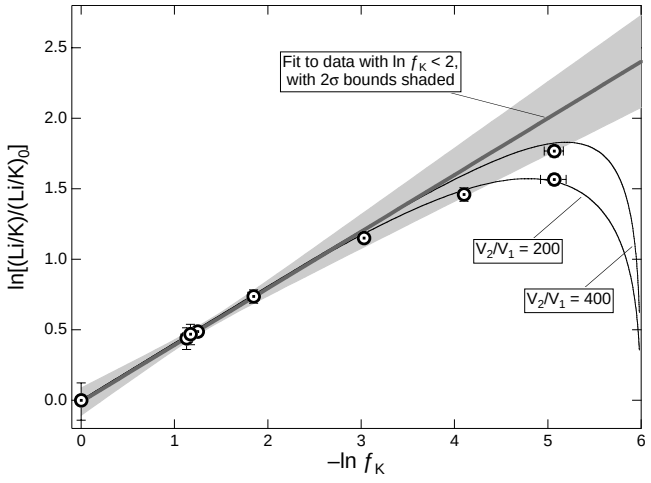

Fig. 2. Change in the Li/K of the inner(source) container as a function of the fraction f_{K} of K remaining, plotted in the manner suggested by Eq. (8). The data, along with 2σ error bars, used to construct this figure are given in an appendix. The heavy straight line is a best fit through the data points with $-\ln f_{\mathrm{K}} \leqslant 1.85$, which were not affected by the finite size of the sink container. Also shown are two thin curves illustrating the effect of the finite size of the sink on the Li/K evolution calculated using Eqs. (4) and (5). The slope of the heavy line corresponds to $D_{\mathrm{Li}}/D_{\mathrm{K}} = 0.598$ and the shading around the straight line shows the 95% confidence limits on the slope (±0.006). The best fitting straight line and the uncertainty of the slope were calculated using Isoplot 3.00 (Ludwig, 2003) taking into account both the precision of the individual data points and the scatter around a best fitting straight line.

two binary systems and use data given in Robinson and Stokes, 1959 for the self-diffusion of Li, K, and Cl in dilute aqueous solutions to calculate the ratio of the diffusivities of Li and K. Self-diffusion coefficients do not take into account that in experiments such as ours, electroneutrality requires that Cl^- diffuse along with the Li^+ and K^+, and therefore each ion cannot have an independent diffusivity. Any perturbation of the flux of the cations relative to the anion will set up an electrostatic force field that will act to restore electroneutrality and thus not allow cations and anions to move independently. The anions and cations must reach a compromise, which expanding on the development given by Cussler (1997) can be derived as follows. The equation for the flux of a singly charged cation i can be written as

$$J_i = -\mathscr{D}_i\left(\nabla C_i + C_i\frac{\Im\nabla\psi}{RT}\right), \quad i = \text{Li or K}, \tag{10}$$

while that for the anion is

$$J_{Cl} = -\mathscr{D}_{Cl}\left(\nabla C_{Cl} - C_{Cl},\frac{\Im\nabla\psi}{RT}\right), \tag{11}$$

where the $\mathscr{D}$'s are self-diffusion coefficients, $\Im$ is Faraday's constant, ψ is the electrostatic potential, R is the gas constant, and T is absolute temperature. We require electroneutrality ($C_{Li} + C_K + C_{Cl} = 0$) and no net electric current ($J_{Li} + J_K + J_{Cl} = 0$) and define a parameter $\alpha = C_K/C_{Li}$ for the concentration ratio of the cations. These constraints can be used to eliminate $\Im\nabla\psi/RT$ resulting in new expressions for the fluxes:

$$J_{Li} = -\left\{\frac{2(1+\alpha)\mathscr{D}_{Li}\mathscr{D}_{Cl}}{(1+\alpha)\mathscr{D}_{Cl} + \mathscr{D}_{Li} + \alpha\mathscr{D}_K}\right\}\nabla C_{Li} \tag{12}$$

and

$$J_K = -\left\{\frac{2(1+\alpha)\mathscr{D}_K\mathscr{D}_{Cl}}{(1+\alpha)\mathscr{D}_{Cl} + \mathscr{D}_{Li} + \alpha\mathscr{D}_K}\right\}\nabla C_K, \tag{13}$$

where the quantities in brackets are the effective diffusion coefficients D_{Li} and D_K for Li and K when Cl is the co-diffuser. What is of interest here, however, is the ratio of the fluxesJ_{Li}/J_K, which turns out (somewhat surprisingly, perhaps) to depend on the ratio of the self-diffusion coefficients (i.e., $D_{Li}/D_K = \mathscr{D}_{Li}/\mathscr{D}_K$) despite the fact that the effective diffusion coefficients for Li and K are not the same as their self-diffusion coefficients.

We can estimate of the ratio of the self-diffusion coefficients of Li and K at 75 °C using the Nernst equation for the limiting self-diffusion coefficients $\mathscr{D}_i = RT\lambda_i/|Z_i|\mathscr{F}^2$, where R is the gas constant, T is absolute temperature, λ_i is the limiting equivalent conductivity of ion i of change Z_i, and $\mathscr{F}$ is the Faraday constant. It follows that $\mathscr{D}_{Li}/\mathscr{D}_K = \lambda_{Li}/\lambda_K$, which we evaluate at $T = 75$ °C by interpolating the limiting equivalent conductivity data given in Appendix 6.2 of Robinson and Stokes (1959). This results in a value of $\mathscr{D}_{Li}/\mathscr{D}_K = 0.58$, which is in reasonably good agreement with the ratio $\mathscr{D}_{Li}/\mathscr{D}_K = 0.598$ derived from the slope of the data in Fig. 2 for $-\ln f \leqslant 1.85$. This agreement, together with the fact that the data in Fig. 2 for $-\ln f \leqslant 1.85$ fall on a straight line (as required by Eq. (9)), is taken as evidence that our experimental design provides an effective way for measuring the ratio of the diffusivities of ions in water. The fact that K diffuses in water considerably faster than Li despite its larger ionic radius and greater mass than Li is evidence of the special nature of ionic diffusion in water, and stands in marked contrast to the behavior in other liquids (e.g., molten silicates) in which Li diffuses orders of magnitude faster than K (Richter et al., 2003).

4.2. $MgCl_2$ experiments

A number of exploratory 75 °C $MgCl_2$ diffusion experiments (Table A1) were run to determine reasonable run durations and the range of associated isotopic fractionations of Mg. Fig. 3 shows that when we plot the natural logarithm of the measured Mg concentrations as a function of time from these experiments the data points fall, with some scatter, along a downward sloping line as required by Eq. (6). Using typical values for the various quantities in the exponent in Eq. (6) ($A = 0.0078$ cm^2, $V \sim 0.6$ cm^3, $L = 0.8$ cm) and the slope (3.67×10^{-7} s^{-1}) of the best fitting line in Fig. 3 results in an estimate of $D \sim 2.3 \times 10^{-5}$ cm^2 s^{-1}. This is in reasonably good agreement with a value of $D = 2.7 \times 10^{-5}$ cm^2 s^{-1} at $T = 75$ °C, which we derived using the Stokes-Einstein relationship in the form $(D\eta/T)_{75\,°C} = (D\eta/T)_{25\,°C}$ together with D=1.16×10^{-5} cm^2 s^{-1} for dilute $MgCl_2$ at 25 °C given in Appendix 11.1 of Robinson and Stokes (1959), and the viscosity η of water at 25 and 75 °C given in Appendix 1.1 of Robinson and Stokes (1959). The use of the Stokes–Einstein relationship to account for the effect of temperature on the diffusivity of ions in water is discussed and justified

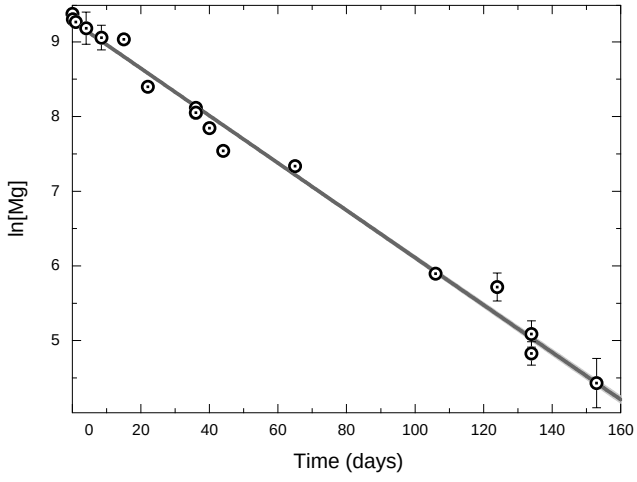

Fig. 3. Natural logarithm of the magnesium concentration of the stating solution and in fluid taken from source chambers plotted as a function of time in days. The data used in this figure are given in Table A1 in appendix. The slope of the best fitting straight line (0.0317) and the 2σ uncertainty (±0.0004) were calculated using Isoplot 3.00 (Ludwig, 2003).

in Li and Gregory (1974). The scatter of the data around the line in Fig. 3 is significantly larger than the analytical uncertainty of the data and it is mainly due to small differences in the internal volume (0.6 ± 0.1 cm^3) of the various source chambers used in our experiments. This limits the precision with which we can determine individual diffusion coefficients, however, as we noted earlier, small differences in the source chambers do not adversely affect the precision of our determinations of the ratio of diffusion coefficients.

The measurements of the isotopic composition of Mg in fluids from these preliminary experiments (see Table A1) were of relatively low precision ($\sim 1‰$, 2σ) and did not resolve any statistically significant isotopic fractionation between the Mg of the starting solution and that of the Mg remaining in the source chamber, or of the Mg that had diffused into the outer chamber. This led us to undertake a new series of diffusion experiments with a variety of conditions ($MgCl_2$ in water diffusing into pure water, and $MgCl_2$ in water containing 0.5% agarose gel diffusing into pure water, $MgCl_2$ diffusing into an outer container containing an approximately equal molar concentration of $CaCl_2$) and used improved analytical procedures to measure the Mg isotopic composition of the solutions with greater precision. The resulting data are given in Table A2 of the Appendix A and plotted in Fig. 4. Even with the higher precision of the new isotopic measurements there is still no resolvable isotopic fractionation of Mg in any of the solutions from these experiments. The precision of the isotopic analyses together with the scatter of the data around a best fitting straight line results in a bound on the isotopic fractionation factor per atomic mass unit of Mg diffusing in water of $\alpha = 1.000032 \pm 0.000061(2\sigma)$.

4.3. Li isotopic fractionation

The isotopic fractionation of Li as it diffuses in water was measured in a series of experiments in which the source container was initially loaded with a LiCl solution ($\sim$0.1 M) and then allowed to diffuse into an outer container filled with pure water. The conditions and compositional data are given in Table A2 of the appendix. Fig. 5 shows the isotopic fractionation of Li as a function of the fraction of Li remaining in the source container plotted in the manner suggested by Eq. 8. The slope of the data in Fig. 5 corresponds to $1000(\{D_{^7\mathrm{Li}}/D_{^6\mathrm{Li}}\} - 1)$ and determines $D_{^7\mathrm{Li}}/D_{^6\mathrm{Li}} = 0.99772 \pm 0.00026(2\sigma)$, which in terms of the exponent β in Eq. (1) corresponds to $\beta = 0.01475$ when $m_1 = 7$ and $m_2 = 6$. Also shown in Fig. 5 is a calculated curve that takes into account the concentration and isotopic composition of Li in the outer container (i.e., using Eq. (5) for the evolution of the inner and outer chambers with Eq. (4) specifying the flux between them). The calculated curve shows that once the fraction of Li remaining in the source container becomes sufficiently small, the isotopic fractionation is expected to fall increasingly below the straight line. For reasons we do not understand, even the most fractionated composition still falls on the same line as the other data points. One possible explanation for this lack of sensitivity to the concentration of Li in the outer container is that it became stratified with the denser, salty fluid ponding at the bottom of the container while the water at the level of the opening of the source container remained relatively fresh (i.e., salt free). Fig. 6 shows a different way of displaying the Li isotopic data from the source container along with three measurements of the Li isotopic composition in the outer container. The

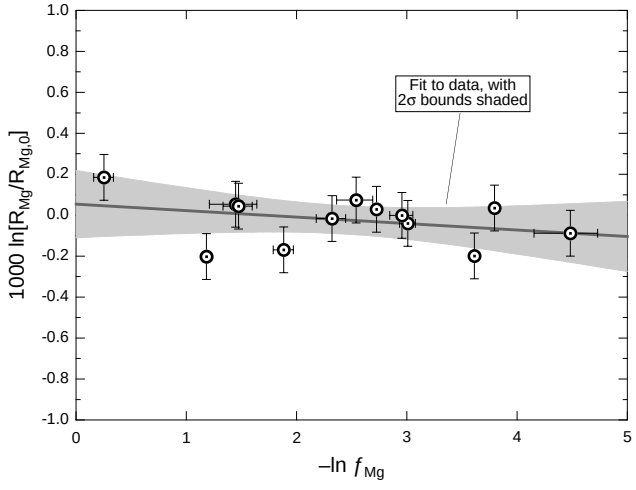

Fig. 4. Same as Fig. 2 but for the change in Mg isotopes as a function of the fraction f_{Mg} of Mg remaining in the source container. The data used in this plot are a combination of the measured $^{25}Mg/^{24}Mg$ and $^{26}Mg/^{24}Mg$ such that each point corresponds to the average Mg isotope fractionation per atomic mass unit ($R_{Mg} = [^{25}Mg/^{24}Mg + (^{26}Mg/^{24}Mg)/2]/2$). The slope of the best fitting line given in Table 1 is not significantly different from zero at the 95% confidence level. The data used in this figure are given in Table A2 of the appendix.

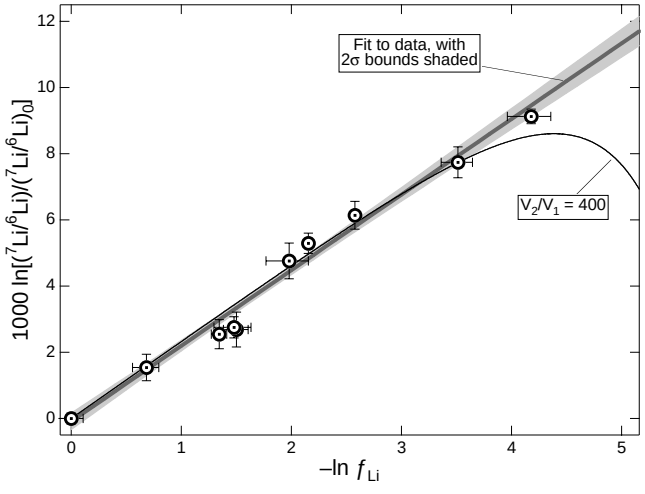

Fig. 5. Same as Fig. 2 but for the change in the ^{7}Li/ ^{6}Li as a function of the fraction f_{Li} of Li remaining in the source flask. The calculated finite-volume evolution curve assumes the largest reasonable ratio of the volumes of the sink and source. The slope of the straight line and the associated 95% confidence limits correspond to $D_{^7\mathrm{Li}}/D_{^6\mathrm{Li}} = 0.99772 \pm 0.00026(2\sigma)$. The data used in this figure are given in Table A2 of the appendix.

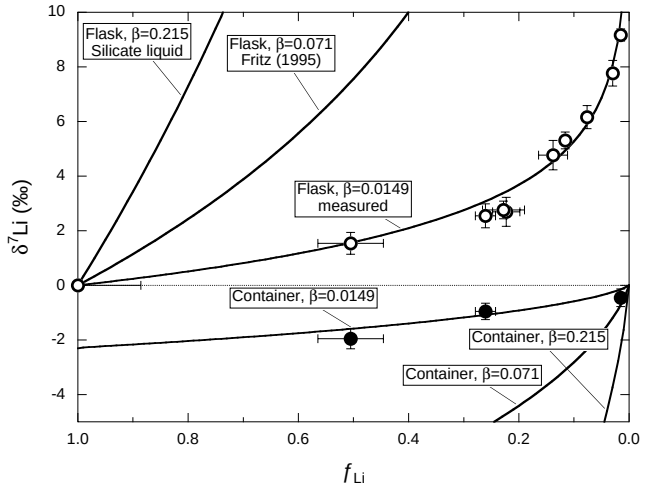

Fig. 6. Same data(open symbols) shown in Fig. 5, but now plotted in terms of the isotopic fractionation of the source reservoir as a function of the fraction f_{Li} of Li remaining in the source. The filled symbols represent three measurements of the Li isotopic composition of the sink reservoir. Model curves were calculated for various choices of the fractionation parameter β in Eq. (1), which determines the ratio of diffusion coefficients used in Eq. (7). The model curves highlight the distinctiveness of our results from those reported by Fritz (1992) and from the fractionation of Li isotopes by diffusion in silicate liquids reported by Richter et al. (2003). The corresponding evolution curves for the sink reservoir are also shown.

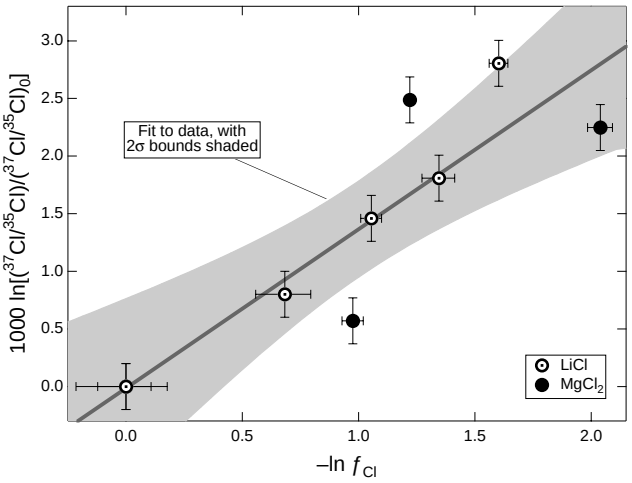

Fig. 7. Same as Fig. 2 but for the change in $^{37}Cl/^{35}Cl$ as a function of the fraction f_{Cl} of Cl remaining in the source container. The slope and 95% confidence limits of the entire data set correspond to $D_{37Cl}/D_{35Cl} = 0.99857 \pm 0.00080$. The data used in this figure are given in Table A2 of the appendix.

isotopic composition is now reported as $\delta^7Li‰ \equiv 1000\left(\{(^7Li/^6Li)_{sample}/(^7Li/^6Li)_o\} - 1\right)$, where the subscript o indicates the starting solution. The figure also includes calculated curves based on Eq. (8) where the ratio of the diffusivities was calculated using Eq. (1) with $\beta = 0.01475$ (for our data), $\beta = 0.071$ (the value corresponding to the Li fractionation reported by Fritz, 1992), and $\beta = 0.215$ (the value reported by Richter et al. (2003) for Li diffusing in a molten silicate liquid). The question of why our data indicate so much less fractionation than those reported by Fritz (1992) is addressed in a later section.

4.4. Cl isotopic fractionation

A subset of the waters taken from the inner container of experiments involving $MgCl_2$ and LiCl was measured for their Cl isotopic composition. The data are given in Table A2 of the appendix and plotted in Figs. 7 and 8. We found $D_{37Cl}/D_{35Cl} = 0.99857 \pm 0.00080(2\sigma)$. For reasons we do not yet fully understand, the data in Figs. 7 and 8 are more scattered around the best fitting straight line than one would expect based on the precision of the individual Cl isotopic measurements, and this scatter accounts for the large uncertainty in our estimate of D_{37Cl}/D_{35Cl}. Nevertheless, the first order result is that diffusion in water fractionates Cl isotopes by a measurable amount regardless of whether the isotopes of the co-diffuser are themselves fractionated. Our results for the fractionation of Cl isotopes by diffusion of LiCl and $MgCl_2$ in water are comparable to the experimental results for Cl isotope fractionation during

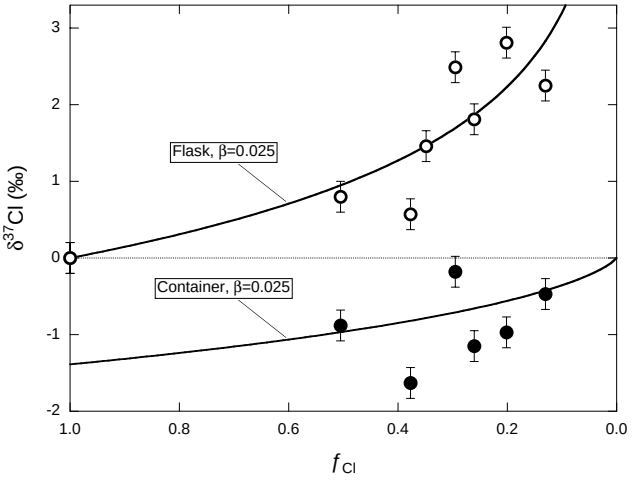

Fig. 8. Same as Fig. 6 but for the Cl isotope data.

diffusion of NaCl in water reported by Coleman and coworkers ($D_{37Cl}/D_{35Cl} = 0.9981$–$0.9986$) at the 2000 Goldschmidt Conference (Coleman et al., 2000). Our results are also within the range of the D_{37Cl}/D_{35Cl} values (0.9970–0.9988) estimated from measurements of Cl isotope ratios in sedimentary pore waters in a variety of natural settings (Desaulniers et al., 1986; Eggenkamp et al., 1994; Groen et al., 2000; Hesse et al., 2000).

5. Discussion

Our results for the isotopic fractionation of Li, Mg, and Cl by diffusion in water are summarized in Table 1. For comparison, we also include the results of various earlier isotope fractionation experiments involving water and molten silicate liquids.

The results from our LiCl–KCl diffusion experiments reproduce the well-known result that lithium, despite its

smaller mass and smaller ionic radius compared to potassium, diffuses significantly slower than potassium (Fig. 2). This result is an indication of the special nature of ionic diffusion in water compared to diffusion in other liquids such as molten silicates. The contrast in diffusive behaviors in water and silicate liquids is dramatic in that in a silicate melt the diffusion coefficient of lithium is two to three orders of magnitude larger than that of potassium and the diffused lithium is far more isotopically fractionated than what we observed in water. The special nature of ionic diffusion in water derives from a variety of sources including solvation and dielectric effects (Hubbard and Onsager, 1977). The effect of hydrodynamic friction is proportional to the radius of the diffusing species, and one can,if one chooses, use the measured ion mobilities to calculate effective radii, which in turn can be rationalized in terms of hydration numbers (i.e., the number of water molecules bound to a solute). Cussler (1997, Table 6.3-1) reports hydration numbers derived from diffusion for Li^+ of 1.3 and for K^+ of −0.1. Hydration numbers derived in this way would seem to be little more than a restatement of the diffusion data in terms of a new set of parameters that are not independently verified, and in fact, these hydration numbers are significantly at odds with the hydration numbers of about 4–6 for Li^+ and K^+ derived by other methods such as neutron scattering (see the review by Enderby, 1995) and molecular computations (see, for example, Rempe et al., 2000; Koneshan et al., 1998). The fact that potassium diffuses significantly faster than lithium in water is most likely the result of dielectric friction that according to continuum models such as that given by Hubbard and Onsager (1977) depends inversely on some power, typically 3, of the radius of the solute. This inverse relationship between size and dielectric friction will have the effect of reducing the mobility of the smaller species, which is opposite the effect of size on the hydrodynamic friction. For charged species, it appears that the dielectric friction dominates in that the experimentally measured mobility of like-charged ions decreases with decreasing ionic radius, as we found for the diffusion of Li^+ and K^+. It is not clear how one would use this way of rationalizing the relative mobility of dissolved ions to derive an expectation for the relative mobility of isotopically distinct species. One would, however, be tempted to believe that the small to negligible isotopic fractionations associated with diffusion in water are the result of hydration. Thinking in terms of a relationship such as given by Eq. (1) where the ratio of the diffusivities of isotopically distinct species is a function of the ratio of the respective masses, hydration, by increasing the effective masses, will reduce the mass ratio and the associated ratio of the diffusivities.

Our focus on high-precision measurements of the relative mobility of isotopes distinguishes the work reported here from most of the earlier work on ion diffusion in water. We found the differences in the mobility of the isotopes of a given ion in water to be surprisingly small compared to mass-dependent effects in other liquids such as molten silicates (see Table 1). The potential role of hydration can be explored by calculating the number of water molecules that would be required to produce an effective mass for the diffusing species such that Eq. (1) will yield the measured ratio of the diffusivities of the isotopically distinct species. The results of such a calculation are given in Table 2 for a range of choices for the exponent β based on values found in other condensed systems that fractionate isotopes by diffusion. In the case of Li the calculation shows that a reasonable number of water molecules together with a plausible value for β (0.215, as found in silicate liquids) can account for the observed isotopic fractionation. In the case of Mg, however, the number of water molecules required is absurdly large even for β as small as 0.075 (the value for Ca isotope fractionation in silicate liquids). Both X-ray diffraction and molecular dynamics calculations find that the coordination shell of Mg^{2+} is made up of six water molecules (Skipper et al., 1989) and thus there is no independent evidence for the very large numbers of waters listed in Table 2. The number of water molecules needed to account for the fractionation of Cl isotopes is also large compared to the number of waters in the first coordination shell (∼6) found by neutron scattering (Enderby, 1995). It seems difficult to avoid the conclusion that the degree of hydration of ions indicated by scattering studies and molecular dynamics calculations does not provide a simple or consistent explanation for the small degree of mass-dependent fractionation of isotopically distinct species as they diffuse in water.

Perhaps, the most important result of the present study is that we have found a much smaller isotopic fractionation of Li by diffusion in water than was reported in an earlier study by Fritz (1992). The magnitude of the difference between these two reports is clearly illustrated in Fig. 6. We are quite confident of our own result in that we have independent evidence from our LiCl–KCl experiments that our experimental design yields accurate relative diffusion coefficients. One difference between Fritz's (1992) experiments and ours is the temperature at which they were run, 25 versus 75 °C. We think it unlikely that temperature effects are the reason for the different degrees of isotopic fractionation found in the two sets of experiments, given that the fractionations reported by Kunze and Fuoss (1962), which are from experiments run at 25 °C, are much more consistent with our results than with those of Fritz (1992). The most likely explanation of why Fritz (1992) found much larger Li isotopic frac-

Table 2
Number of waters of hydration (n) such that when the combined mass of the isotopes plus water is used in Eq. 1 together with a choice of β, the calculated ratio of the diffusivities of the isotopically distinct species corresponds to the measured value D_i/D_j

	$\beta = 0.5$	$\beta = 0.215$	$\beta = 0.075$	D_i/D_j
$Li + nH_2O$	12	5	1.5	0.99772
$Mg + nH_2O$	900	400	140	>0.99997
$Cl + nH_2O$	37	15	4	0.99857

tionation than what we measured is that his experimental design allowed for processes other than diffusion in water. In Fritz's (1992) experiment, the volume of water containing dissolved LiCl was enclosed in a dialysis membrane and the diffusion out of that volume was through the membrane. The exciting prospect is that Fritz's results, when contrasted with ours, may be telling us that transport of ions across membranes can effect isotopic fractionations that are much larger than those which take place by diffusion in water itself. The obvious test of this hypothesis is to design experiments that focus on mass-dependent isotopic fractionation by transport across membranes. The results of such experiments may prove to be quite relevant for developing a better understanding of the isotopic fractionation by organisms such as the foraminifera studied by Gussone et al. (2003).

Acknowledgments

We thank Erick Ramon for ICPMS analyses of Mg concentrations in our experimental solutions. We also thank Andy Davis of the University of Chicago for his help with the analysis and presentation of the data and Richard Zeebe of the University of Hawaii for his detailed and very helpful review of the original version of this paper. F.M.R.'s participation in this work was supported by DOE Grant DE-FG02-ER15254. The work by I.D.H. and R.W.W. was performed under the auspices of the US Department of Energy by the University of California, Lawrence Livermore National Laboratory under Contract No. W-7405-Eng-48.

Associate editor: Juske Horita

Appendix A

Sample designations in Tables A1 and A2 include the letters S of L to indicate short (0.8 cm) or long (1.2 cm) diffusion tube length, F or C to indicate source flask or outer container, and numbers preceding D to indicate the duration of the experiment in days.

Table A1
$MgCl_2$, $T = 75$ °C

Sample	Time in days	Mg (ppm)	2σ	δ^{25}Mg source flask	δ^{25}Mg outer container
Starting sol.	0	11,807	554	2.28	
07S7-F0.1D	0.1	10,977	405	1.98	2.63
07S7-F1D	1	10,586	455	2.54	2.71
07S5-F4D	4	9729	2343	2.36	2.28
07S9-F8.5D	8.5	8587	1548		
07S1-F15D	15	8405	480		
07S4-F22D	22	4452	206	2.97	3.01
07S1-F36D	36	3353	192	2.15	1.96
07S9-F36D	36	3136	161	1.80	2.50
07S5-36D	36	3141	218	2.12	1.89
07S3-F40D	40	2558	135		
07S7-44D	44	1885	110	2.51	2.49
07S2-F65D	65	1536	41	2.67	2.50
07S3-F106D	106	364	16	1.67	1.75
07S5-F124D	124	304	63		
07S3-F134D	134	125	21		
07S4-F134D	134	162	31		
07S8-F153D	153	84	33		

Table A2
LiCl+KCl, $T = 75$ °C

Sample	n	Li ppm	2σ	K ppm	2σ
Starting sol.	5	352.6	13.6	1875.4	37.8
07L2-F-41D	4	165.1	1.8	538.8	10.8
07L-F-5-53D	3	176.9	5.9	606.4	21.6
07S2-F-41D	4	116.1	2.1	295.6	9.4
07L-F-9-81D	3	53.9	1.5	90.7	2.1
07S5-F-53D	3	174.6	6.8	581.3	15.9
07S8-F-1-81D	3	25.1	2.5	31	0.6
07S10-F-108D	3	13.5	1.4	15.1	0.1
07L10-F-160D	3	13	1.0	11.8	0.9

(*continued on next page*)

Table A2 (*continued*)
Li isotope fractionation, $T = 75$ °C

Sample	Li (ppm)	2σ	δ^7Li	2σ
Starting sol.	763.4	87.2	0	0.17
07L5-F-31D	385.6	45.4	1.54	0.4
07L3-F-58D	170.1	19	2.69	0.53
07L-D-F-84D	58.0	2.28	6.16	0.42
07L1-F-99D	173.8	29	2.76	0.32
07S5-F-31D	198.8	14	2.55	0.44
07S3-F-58D	88.5	3.6	5.31	0.31
07S6-F-99D	11.7	2.28	9.17	0.22
07S4-F-74D	22.8	3.2	7.77	0.47
07L7-F-74D	105.3	20	4.77	0.54
Container samples				
07L5-C-31D			−1.95	0.37
07S5-C-31D			−0.95	0.3
07S6-C-99D			−0.45	0.32

Cl isotope fractionation, $T = 75$ °C

			flask samples		Container samples	
LiCl	Li (ppm)	2σ	δ^{37}Cl	2σ	δ^{37}Cl	2σ
Starting sol.	763.4	87.2	0	0.2		
07L5-F-31D	385.6	45.4	0.8	0.2	−0.88	0.2
07S5-F-31D	198.8	14	1.81	0.2	−1.15	0.2
07L2-F-45D	266	10.2	1.46	0.2		
07S10-F-45D	153.7	6.14	2.81	0.2	−0.97	0.2
$MgCl_2$	Mg (ppm)	2σ	δ^{37}Cl	2σ		
Starting sol.	11807	1143	0	0.2		
07S4-F-22D	4452	101	0.57	0.2	−1.63	0.2
07S2-F-65D	1536	41	2.25	0.2	−0.47	0.2
07L10-F-75D	3485	90	2.49	0.2	−0.18	0.2

Mg isotope fractionation, $T = 38°$ and 75 °C

Starting sol.	Mg or Ca (ppm)	2σ	Isotopic fractionation		
$MgCl_2$	2979	314.8			
$CaCl_2$	3942	271.2			
			Flask		Container
Sample	Mg (ppm)	2σ	δ^{25}Mg	δ^{26}Mg	δ^{25}Mg
07S1-F-223D ($MgCl_2 + CaCl_2$)	66.9	2.12	2.31	4.44	
07S2-F-173D ($MgCl_2 + CaCl_2$)	146.9	10.52	2.23	4.31	2.39
07S5-F-223D ($MgCl_2 + CaCl_2$)	33.6	9.46	2.17	4.22	2.46
07L5-F-222D($MgCl_2 + CaCl_2$)	195.3	6.36	2.28	4.48	
07L7-F-222D ($MgCl_2 + CaCl_2$)	80.3	1.12	2.08	3.97	2.55
07L9-F-172D ($MgCl_2 + CaCl_2$)	234.7	38	2.32	4.57	2.17
07S7-F-133D ($MgCl_2$)[a]	155.1	16.2	2.28	4.35	2.23
07S9-F-133D ($MgCl_2 + CaCl_2$)[a]	913.5	26.62	2.03	4.05	2.05
07L3-F-133D ($MgCl_2$)[a]	2314.2[b]	208	2.37	4.91	2.29
07S3-F-133D ($MgCl_2 + CaCl_2$ + agar)[a]	700.5	148	2.31	4.52	2.68
07S6-F-133D ($MgCl_2$ + agar)[a]	292.2	38.8	2.22	4.42	2.32
07L6-F-133D ($MgCl_2$ + agar)[a]	682.2	90	2.28	4.53	2.25
07LD-F-133D ($MgCl_2 + CaCl_2$+agar)[a]	453.0	41.4	2.08	4.08	2.40

2σ external precision 0.2‰ for δ^{25}Mg and δ^{26}Mg. Duplicates generally better than 0.2‰.
[a] $T = 75$ °C except for samples incubated at $T = 38$ °C.
[b] High concentration remaining after 133 days is due to a bubble obstructing the diffusion tube.

References

Coleman, M., Eggenkamp, H., Aranyossy, J.F., **2000**. History of solute transport in a 400 m mudrock sequences, calibrated by laboratory chlorine stable isotope diffusion experiments. Extended abstract from Goldschimdt 2000 in *J. Conf. Abstracts* 5, 313–314.

Craig, H., Gordon, L., 1965. Deuterium and oxygen 18 variation in the ocean and marine atmosphere. In: Tongiorgi (Ed.), *Stable Isotopes in Oceanographic Studies and Paleotemperatures*. Spoleto, CNR, pp. 9–130.

Cussler, E.L., 1997. *Diffusion, Mass Transfer in Fluid Systems*, second ed. Cambridge University Press, Cambridge, MA.

Desaulniers, D.E., Kaufmann, R.S., Cherry, J.A., Bentley, H.W., 1986. ^{37}Cl–^{35}Cl variations in a diffusion controlled groundwater system. *Geochim.Cosmochim. Acta* **50**, 1757–1764.

Eggenkamp, H., **1994**. $\delta^{37}Cl$: The geochemistry of chlorine isotopes. Faculteit Aardwetenschappen, Universiteit Utrecht, Geologica Ultraiectina, No. 116.

Eggenkamp, H.G.M., Middleburg, J.J., Kreulen, R., 1994. Preferential diffusion of ^{35}Cl relative to ^{37}Cl in sediments of Kau Bay, Halmahera, Indonesia. *Chem. Geol.* **116**, 317–325.

Enderby, J.E., 1995. Ion solvation via neutron scattering. *Chem. Soc. Rev.* **24**, 159–168.

Fritz, S.J., 1992. Measuring the ratio of aqueous diffusion coefficients between $^{6}Li^{+}Cl^{-}$ and $^{7}Li^{+}Cl^{-}$ by osmometry. *Geochim. Cosmochim. Acta* **56**, 3781–3789.

Galy, A., Yoffe, O., Janney, P.E., Williams, R.W., Cloquet, C., Alard, O., Halicz, L., Wadhwa, M., Hutcheon, I.D., Ramon, E., Carignan, J., 2003. Magnesium isotopes heterogeneity of the isotopic standard SRM980 and new reference materials for magnesium-isotope-ratio measurements. *J. Anal. At. Spectrom.* **18**, 1352–1356.

Groen, J., Velstra, J., Meesters, A.G.C.A., 2000. Salinization processes in paleowaters in coastal sediments of Suriname: Evidence from $\delta^{37}Cl$ analysis and diffusion modeling. *J. Hydrol.* **234**, 1–20.

Gussone, N., Eisenhauer, A., Heuser, A., Dietzel, M., Bock, B., Böhm, F., Spero, H.J., Lea, D.W., Bijma, J., Nägler, T.F., 2003. Model for kinetic effects on calcium isotope fractionation ($\delta^{44}Ca$) in inorganic aragonite and cultured planktonic foraminifera. *Geochim. Cosmochim. Acta* **67**, 1375–1382.

Hesse, R., Frape, S.K., Egeberg, P., Matsumoto, R., **2000**. Stable isotope studies(Cl, O, and H) of interstitial waters from Site 997, Blake Ridge gas hydrate field, West Atlantic. In: Paull, C.K., Matsumoto R.,Wallace P.J., Dillon W.P. (Eds.), *Proceedings of the Ocean Drilling Program, Scientific Results* 164, pp. 129–137.

Holt, B.D., Sturchio, N.C., Abrajano, T.A., Heraty, L.J., 1997. Conversion of volatile chlorinated organic compounds to carbon dioxide and methyl chloride for isotopic analysis of carbon and chlorine. *Anal. Chem.* **69**, 2727–2733.

Hubbard, J., Onsager, L., 1977. Dielectric dispersion and dielectric friction in electrolyte solutions. *J. Chem. Phys.* **67**, 4850–4857.

Jähne, B., Heinz, G., Dietrich, W., **1987**. Measurements of diffusion coefficients of sparingly soluble gases in water. *J. Geophys. Res.* 92, 10,767–10,776.

Koneshan, S., Jayendran, C.R., Lynden-Bell, R.M., Lee, S.H., 1998. Solvent structure, dynamics, and ion mobility in aqueous solutions at 25 °C. *J. Phys. Chem.* **102**, 4193–4204.

Kunze, R.W., Fuoss, R.M., 1962. Conductance of the alkali halides. III. The isotopic lithium chlorides. *J. Phys. Chem.* **66**, 930–931.

Leaist, D.G., Kanakos, M.A., 2000. Measured and predicted ternary diffusion coefficients for concentrated aqueous LiCl + KCl solution over a wide range of compositions. *Phys. Chem. Chem. Phys.* **2**, 1015–1021.

Li, Y.-H., Gregory, S., 1974. Diffusion of ions in seawater and in deep-sea sediments. *Geochim. Cosmochim. Acta* **38**, 703–714.

Ludwig, K.R., **2003**. User's manual for Isoplot 3.00: A Geochronological Toolkit for Microsoft Excel.Berkeley Geochronology Center Special Publication No. 4, Berkeley, California.

Pikal, M.J., 1972. Isotope effects in tracer diffusion. Comparison of the diffusion coefficients of $^{24}Na^{+}$ and $^{22}Na^{+}$ in aqueous electrolytes. *J. Phys. Chem.* **76**, 3038–3040.

Prinzhofer, A., Pernaton, E., 1997. Isotopically light methane in natural gas: bacterial imprint or diffusive frsactionation? *Chem. Geol.* **142**, 193–200.

Rempe, S.B., Pratt, L.R., Hummer, G., Kress, J.D., Martin, R.L., Redondo, A., 2000. The hydration number of Li^{+} in liquid water. *J. Am. Chem. Soc.* **122**, 966–967.

Richter, F.M., Liang, Y., Davis, A.M., 1999. Isotope fractionation by diffusion in molten oxides. *Geochim. Cosmochim. Acta* **63**, 2853–2861.

Richter, F.M., Davis, A.M., DePaolo, D.J., Watson, E.B., 2003. Isotope fractionation by chemical diffusion between molten basalt and rhyolite. *Geochim. Cosmochim. Acta* **67**, 3905–3923.

Robinson, R.A., Stokes, R.H., **1959**. Electrolyte Solutions, second ed. Butterworths, London, 559 pp.

Rodushkin, I., Stenberg, A., Andrén, H., Malinovsky, D., Baxter, D.C., 2004. Isotopic fractionation during diffusion of transition metal ions in solution.Anal. *Chemistry* **76**, 2148–2151.

Skipper, N.T., Neilson, G.W., Cummings, S.C., 1989. An X-ray diffraction study of $Ni^{2+}_{(aq)}$ and $Mg^{2+}_{(aq)}$ by difference methods. *J. Phys. Condens. Matter* **1**, 3489–3506.

Zhang, T., Krooss, B.M., 2001. Experimental investigation of on the carbon isotope fractionation of methane during gas migration by diffusion through sedimentary rocks at elevated temperatures and pressure. *Geochim. Cosmochim. Acta* **65**, 2723–2742.